



LJMU Research Online

Arevalillo-Herráez, M, Gdeisat, M, Lilley, F and Burton, DR

A spatial algorithm to reduce phase wraps from two dimensional signals in fringe projection profilometry

<http://researchonline.ljmu.ac.uk/id/eprint/3438/>

Article

Citation (please note it is advisable to refer to the publisher's version if you intend to cite from this work)

Arevalillo-Herráez, M, Gdeisat, M, Lilley, F and Burton, DR (2016) A spatial algorithm to reduce phase wraps from two dimensional signals in fringe projection profilometry. Optics and Lasers in Engineering, 82. pp. 70-78. ISSN 0143-8166

LJMU has developed **LJMU Research Online** for users to access the research output of the University more effectively. Copyright © and Moral Rights for the papers on this site are retained by the individual authors and/or other copyright owners. Users may download and/or print one copy of any article(s) in LJMU Research Online to facilitate their private study or for non-commercial research. You may not engage in further distribution of the material or use it for any profit-making activities or any commercial gain.

The version presented here may differ from the published version or from the version of the record. Please see the repository URL above for details on accessing the published version and note that access may require a subscription.

For more information please contact researchonline@ljmu.ac.uk

<http://researchonline.ljmu.ac.uk/>

A spatial algorithm to reduce phase wraps from two dimensional signals in fringe projection profilometry

Miguel Arevalillo-Herráez^{a,1}, Munther Gdeisat^b, Francis Lilley^c, David R. Burton^c

^a*Departament d'Informàtica, Universitat de València. Avda. de la Universidad s/n. 46100-Burjasot, Spain*

^b*Colleges of Applied Sciences, Sohar, PO BOX 135, Post Code 311, Oman*

^c*General Engineering Research Institute, Liverpool John Moores University, Byrom Street, Liverpool, L3 3AF, UK*

Abstract

In this paper, we present a novel algorithm to reduce the number of phase wraps in two dimensional signals in fringe projection profilometry. The technique operates in the spatial domain, and achieves a significant computational saving with regard to existing methods based on frequency shifting. The method works by estimating the modes of the first differences distribution in each axial direction. These are used to generate a tilted plane, which is subtracted from the entire phase map. Finally, the result is re-wrapped to obtain a phase map with fewer wraps. The method may be able to completely eliminate the phase wraps in many cases, or can achieve a significant phase wrap reduction that helps the subsequent unwrapping of the signal. The algorithm has been exhaustively tested across a large number of real and simulated signals, showing similar results compared to approaches operating

Email addresses: Miguel.Arevalillo@uv.es (Miguel Arevalillo-Herráez), Gdeisat@hotmail.com (Munther Gdeisat), f.lilley@ljmu.ac.uk (Francis Lilley), d.r.burton@ljmu.ac.uk (David R. Burton)

in the frequency domain, but at significantly lower running times.

Keywords: phase unwrapping, wrap reduction, frequency shifting, Fourier analysis

1. Introduction

Phase measuring fringe projection profilometry methods attempt to obtain a surface measurement by projecting a sinusoidal fringe pattern onto an object. The height of the object at each point is related to the phase of the deformed fringe pattern. This is usually extracted by using phase retrieval methods [1, 2], such as Fourier [3], wavelet [4], FIR Hilbert transformers [5], Shearlet transforms [6] or phase shifting methods [7].

In all these cases, the retrieved information consists of the principal values, which are bounded in the range $(-\pi, \pi]$. This may cause discontinuities within the phase signal (wraps), which should not be present in the unbounded height measurements. The process of resolving these phase discontinuities is called phase unwrapping, and the process also occurs in various other fields of research, such as in geoscience (SAR radar) and in medicine (MRI scanning). Phase unwrapping has been a matter of extensive research for the last two decades. As a result, many different techniques have been developed to tackle phase unwrapping problems. These include global error minimization algorithms [8, 9], branch-cut methods [10, 11], quality guided techniques [12, 13, 14, 15] and region-growing approaches [16, 17].

Attempts have also been made at reducing the number of fringes in the phase map, to reduce the complexity of the problem. In Fourier profilometry, one way to achieve this is by frequency shifting in the Fourier domain [3, 18].

This approach has been recently extended so that it can be used with other phase retrieval methods [19]. The wrap reduction has a positive effect on the subsequent unwrapping step. However, the method suffers in terms of execution speed from the significant computation involved in the necessary trigonometric operations and the 2D discrete Fourier transform (DFT) that are involved.

In this paper, we present an alternative algorithm that operates in the spatial domain and hence does not require the use of the DFT. The technique resembles the behavior of the frequency shift method [19]. First, the modes of the first differences distribution in each direction are estimated. These are then used to generate a tilted plane, which is subtracted from the entire phase map. Finally, the result is re-wrapped to obtain a phase map that contains fewer wraps. The wrap reduction that is achieved by the proposed approach is similar to that which is obtained by using the frequency shift method, but the new method runs in linear time, so is significantly faster than the method presented in [19]. Potential benefits to unwrapping results are illustrated on both simulated and real fringe patterns.

2. Wrap reduction in the Fourier Domain

Given a wrapped phase signal $\phi_w(x, y)$, the method presented in [19] applies Algorithm 1 to reduce the number of wraps in the phase map. First, the complex signal $\psi(x, y)$ is built, and the 2D Fourier transform operator \mathcal{F} is applied to the result. Then, the indexes for the maximum value in the frequency spectrum, u_0 and v_0 , are determined. These are used to shift the Fourier transform of the complex signal towards the origin. Subsequently, the

inverse Fourier transform of the shifted signal $\Psi'(u, v)$ is computed, to yield $\psi'(x, y)$. Finally, the new phase function $\phi'_w(x, y)$ is extracted by using the four quadrant *arctan* function on the ratio between the real and imaginary parts of signal $\psi'(x, y)$.

- (1) $\psi(x, y) = e^{i\phi_w(x, y)}$;
- (2) $\Psi(u, v) = \mathcal{F}\{\psi(x, y)\}$;
- (3) $u_0, v_0 = \arg \max_{u, v} \text{abs}(\Psi(u, v))$;
- (4) $\Psi'(u, v) = \Psi(u + u_0, v + v_0)$;
- (5) $\psi'(x, y) = \mathcal{F}^{-1}\{\Psi'(u, v)\}$;
- (6) $\phi'_w(x, y) = \arctan\left(\frac{\mathcal{I}(\psi'(x, y))}{\mathcal{R}(\psi'(x, y))}\right)$;

Algorithm 1: Pseudo-code for the wrap reduction algorithm in the Fourier Domain[19] .

When using Fourier Analysis, the function $\Psi(u, v)$ and steps (3)-(6) in Algorithm 1 are an inherent part of the phase retrieval operation. Although the slight loss of accuracy has made some authors ignore the frequency shifting stage in later work, it was actually a step in the original method [18]. In addition, if the shift is combined with carefully designed optics, the technique has the potential to make unwrapping unnecessary [18].

When using other existing phase extraction methods, Algorithm 1 needs to be run entirely. Despite the apparent complexity of the method, it translates into the spatial domain as a removal of a tilted plane, followed by a re-wrap operation to the original bound interval. The slopes of this plane in the x and y directions are $2\pi u_0/N_X$ and $2\pi v_0/N_Y$, respectively, where N_X and N_Y refer to the size of the original wrapped phase signal.

This can be proven by considering the shift property of the Fourier transform: $f(x, y)e^{i2\pi(u_0x/N_X+v_0y/N_Y)} \iff F(u-u_0, v-v_0)$. The function $\psi'(x, y)$ then becomes

$$\begin{aligned}\psi'(x, y) &= \psi(x, y)e^{-i(2\pi u_0x/N_X+2\pi v_0y/N_Y)} \\ &= e^{i(\phi_w(x, y)-2\pi u_0x/N_X-2\pi v_0y/N_Y)}\end{aligned}\tag{1}$$

and the resulting phase map is given by

$$\begin{aligned}\phi'_w(x, y) &= \arctan\left(\frac{\mathcal{I}(\psi'(x, y))}{\mathcal{R}(\psi'(x, y))}\right) \\ &= \arctan\left(\frac{\sin(\phi_w(x, y) - 2\pi u_0x/N_X - 2\pi v_0y/N_Y)}{\cos(\phi_w(x, y) - 2\pi u_0x/N_X - 2\pi v_0y/N_Y)}\right) \\ &= \mathcal{W}(\phi_w(x, y) - 2\pi u_0x/N_X - 2\pi v_0y/N_Y)\end{aligned}\tag{2}$$

where \mathcal{W} stands for the wrapping operator, as a result of the application of the *arctan* function; and \mathcal{R} and \mathcal{I} are used to refer to the real and imaginary part of the argument signal.

The removal of the slope can be easily performed in the spatial domain if u_0 and v_0 are known.

3. Wrap reduction in the Spatial Domain

3.1. Principles

Any local slope that is present in the original phase function $\phi(x, y)$ has an effect on a frequency term in $\Psi(u, v)$. In particular, any slope (k_x, k_y) in

the x- and y-axis, respectively, will contribute to the frequency component $u = k_x N_X / 2\pi, v = k_y N_Y / 2\pi$, in a degree that depends on the size of the region.

Intuitively, this makes it possible to estimate the most common frequency values u_0 and v_0 in Algorithm 1 as being the most frequent slope in the original phase function $\phi(x, y)$. This estimate can easily be produced in a local manner, by computing the mode of the bivariate distribution of the wrapped first differences in the x and y directions at each point. Once values u_0 and v_0 have been computed, the new phase map $\phi'(x, y)$ can be obtained by removing a slope $(2\pi u_0 / N_X, 2\pi v_0 / N_Y)$ and then re-wrapping the result in the original interval $(-\pi, \pi]$.

The consideration of the first differences in the x and y directions as a bivariate distribution aim to maximize the total area of constant regions in the result (pixels with first differences that are equal to zero). This is particularly convenient when the object does not fill the entire image field, i.e. it only comprises part of the 2D phase signal. In this case, the process above usually identifies and cancels out the carrier frequency caused by the pattern projected onto the surface, which was the original aim of the frequency shift [3]. If the purpose is to reduce the number of wraps, there are benefits to considering each direction separately, as can be seen in the following example.

Apart from a computational advantage, a greater wrap reduction can potentially be achieved. Figure 1(a) shows a simulated wrapped phase signal, and Figures 1(b)-(d) illustrate the results obtained with frequency shifting and the proposed spatial method, firstly considering the bivariate distribution of first differences (c); and secondly with one distribution per axial direction

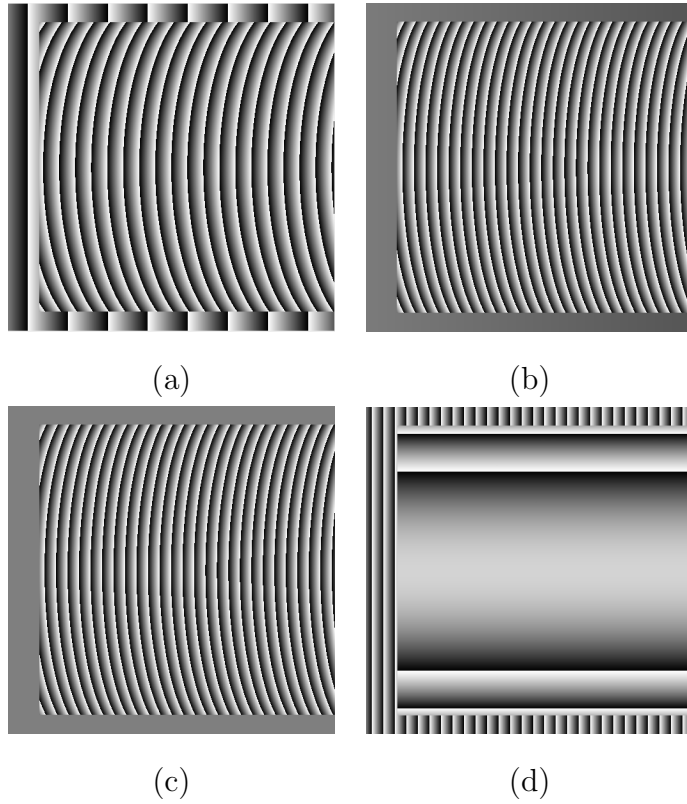


Figure 1: (a) A simulated wrapped phase signal (a), and results obtained by (b) frequency shifting in Fourier space; (c) spatial method using bivariate distribution; and (d) spatial method considering each axial direction separately.

in x and y (d). Figures 1(b) and (c) show that the frequency shifting and spatial algorithms have done their best to maximize the total size of regions of constant value, visible here around the image borders. As a side effect, the number of fringes on the surface has actually increased. On the contrary, when looking for the optimum slope in both axes separately, this has led to a better result on the object's surface, with far less phase wraps being evident.

3.2. Implementation

Algorithm 2 outlines the entire operation of the method proposed. Steps (1), (2) and (5) require the use of the wrapping operator \mathcal{W} . This operator can efficiently be defined as

$$\mathcal{W}(x) = x - 2\pi \lfloor \frac{(x + \pi)}{2\pi} \rfloor \quad (3)$$

with $\lfloor x \rfloor$ the floor function, which maps a real number to the largest integer not greater than x .

- (1) compute horizontal first wrapped differences ;
- (2) compute vertical second wrapped differences ;
- (3) compute the mode for first and second wrapped differences ;
- (4) subtract slopes in x- and y- directions from original phase signal $phi(x, y)$;
- (5) re-wrap the signal using the operator \mathcal{W} ;

Algorithm 2: Pseudo-code for the proposed spatial method .

Mode estimation is a topic that has been extensively researched. As a result many accurate parametric and non-parametric methods exist for this purpose [20, 21]. With a focus on speed, we have used a naive histogram-based estimator, and fixed the number of bins at values between $b = 64$ and $b = 256$. Special care needs to be taken when the wrapped phase signal has been quantized using a comparatively small number of levels relative to the resolution of the spatial phase. High spatial phase resolutions with a low number of quantization levels will very likely yield a zero mode, meaning that the proposed algorithm will have no effect unless the bin size spans several

quantization levels. The computation of the histogram can easily be done in linear time, by making each value x contribute to the bin in position

$$1 + \lfloor b \frac{x + \pi}{2\pi} \rfloor \quad (4)$$

Once the histogram has been computed, one possible estimation of the mode is given by

$$mode = L + \frac{f_0 - f_{-1}}{(f_0 - f_{-1}) + (f_0 - f_{+1})} s \quad (5)$$

with L representing the lower limit of the most frequent histogram bin; and f_0 , f_{-1} and f_{+1} representing the frequencies for the most frequently occurring frequency bin, the previous bin and the next one, respectively. An alternative to this interpolation of frequencies is to consider the average of all the values that contributed to the most frequent bin. However, this requires a second pass through the array of differences to filter the ones within the bin. In the rest of this paper, we will refer to these methods as Histogram Interpolated Mode (HIM) and Histogram Averaged Mode (HAM), respectively.

4. Evaluation

A number of simulations and comparative experiments have been carried out in order to assess the relative merits of the proposed approach in its different aspects and in comparison to the frequency shift method presented in [19]. The two naive estimators of the mode presented in Section 3.2 (HIM and HAM) have also been evaluated in different contexts. Samples presented in this section are a summary of an extensive experimentation regime, and

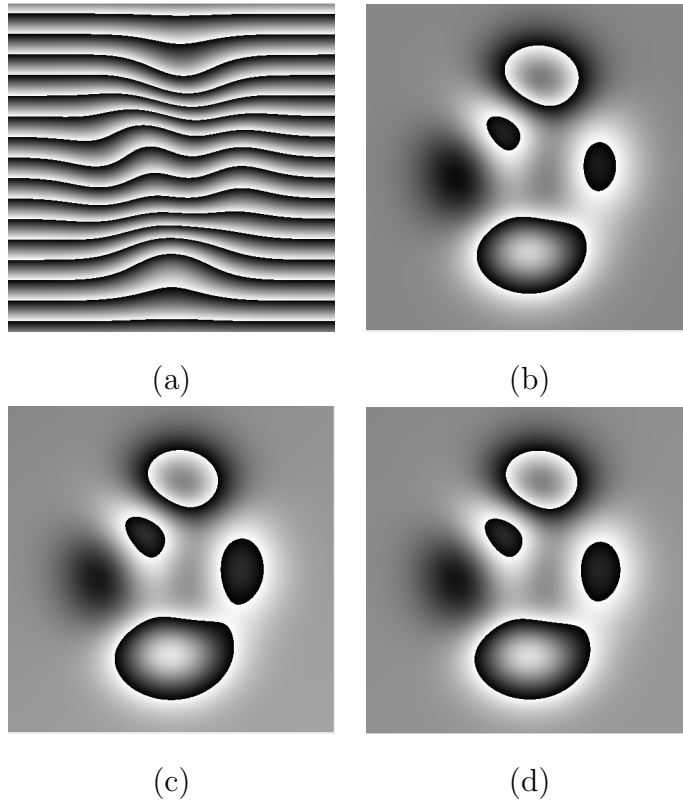


Figure 2: (a) A simulated wrapped phase signal, and results obtained by (b) frequency shifting in Fourier space; (c) spatial method using interpolation on highest frequency bin; and (d) spatial method using average of samples in highest frequency bin

have been selected to outline the benefits and disadvantages of the proposed technique. Results are evaluated with regard to both the level of wrap reduction achieved and the computational execution time.

4.1. Wrap reduction

As the first assessment task, we analyze and compare the results obtained with the three methods on several typical wrapped phase signals. Figure 2 shows a first example on a simulated pattern. The shape corresponds to the

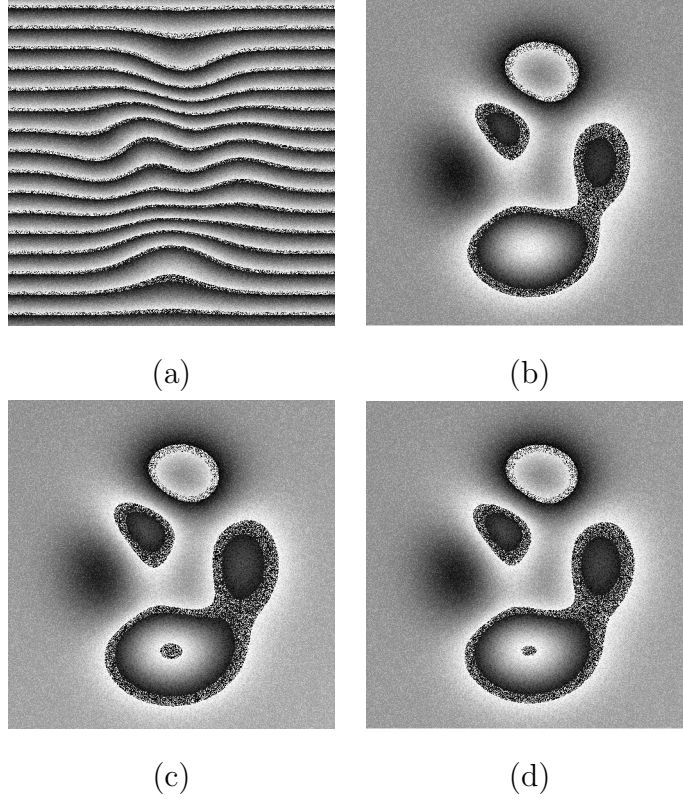


Figure 3: (a) A simulated wrapped phase signal with added noise, and results obtained by (b) frequency shifting in Fourier space; (c) spatial method using interpolation on highest frequency bin; and (d) spatial method using average of samples in highest frequency bin

function

$$\phi(x, y) = 3(1 - x)^2 e^{-x^2 - (y+1)^2} - 10\left(\frac{x}{5} - x^3 - y^5\right) e^{-x^2 - y^2} - \frac{1}{3} e^{-(x+1)^2 - y^2} \quad (6)$$

and has been generated by using the Matlab function peaks and adding a carrier frequency along the y axis. Results show a very similar performance in terms of the three methods, with no significant difference in wrap reduction between them.

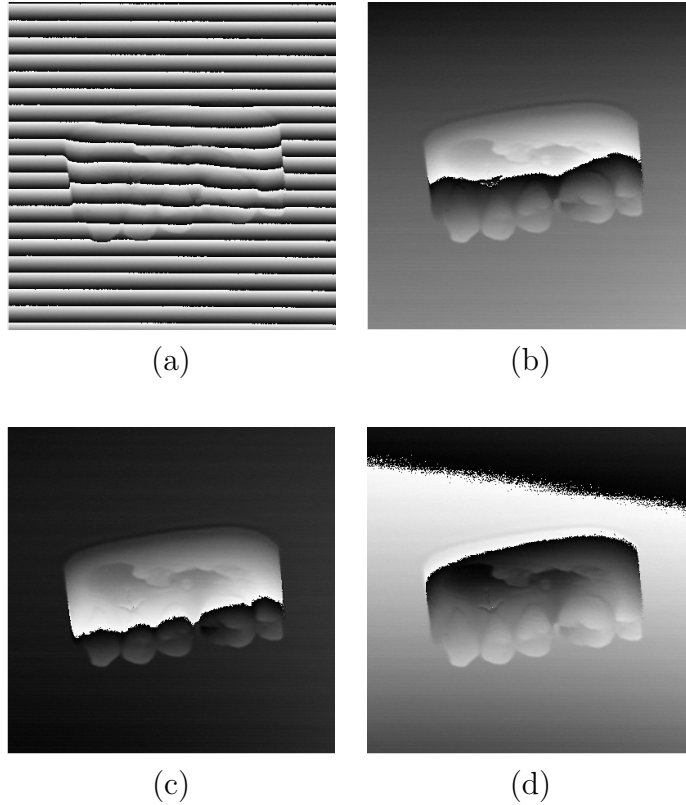


Figure 4: (a) A real wrapped phase signal, and results obtained by (b) frequency shifting in Fourier space; (c) spatial method using interpolation on highest frequency bin; and (d) spatial method using average of samples in highest frequency bin

In order to test the robustness of the methods to global noise in the wrapped signal, we have also tested the results when adding white noise with a variance of 1.1 and a mean of 0 to the pattern shown in Figure 2. The new pattern is presented in Figure 3(a), and results for the three methods are shown in Figure 3(b)-(d). Again, no significant difference is observed in the results.

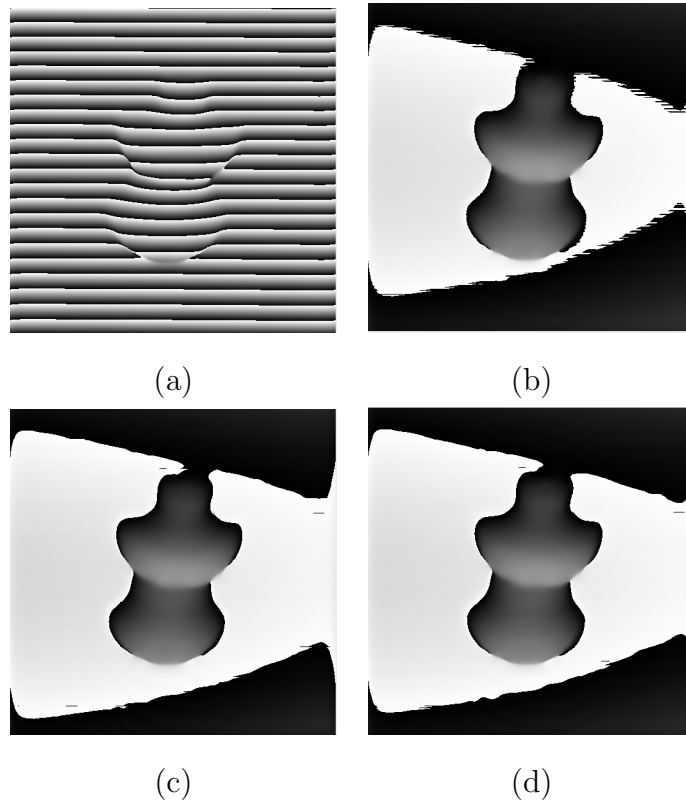


Figure 5: (a) A real wrapped phase signal, and results obtained by (b) frequency shifting in Fourier space; (c) spatial method using interpolation on highest frequency bin; and (d) spatial method using average of samples in highest frequency bin

Figures 4 and 5 correspond to real wrapped phase signals for real object measurement, for a dental cast and a bottle-shaped object respectively. Again, the three methods yield an equivalent level of performance, leaving a single phase wrap in all three cases. Further examples on real fringe patterns are provided in Figures 6, 7 and 8. These have been obtained by using fringe projection on a computer keyboard, a statue of a fairy and a mechanical clutch plate component. The effectiveness of the three methods is quite sim-

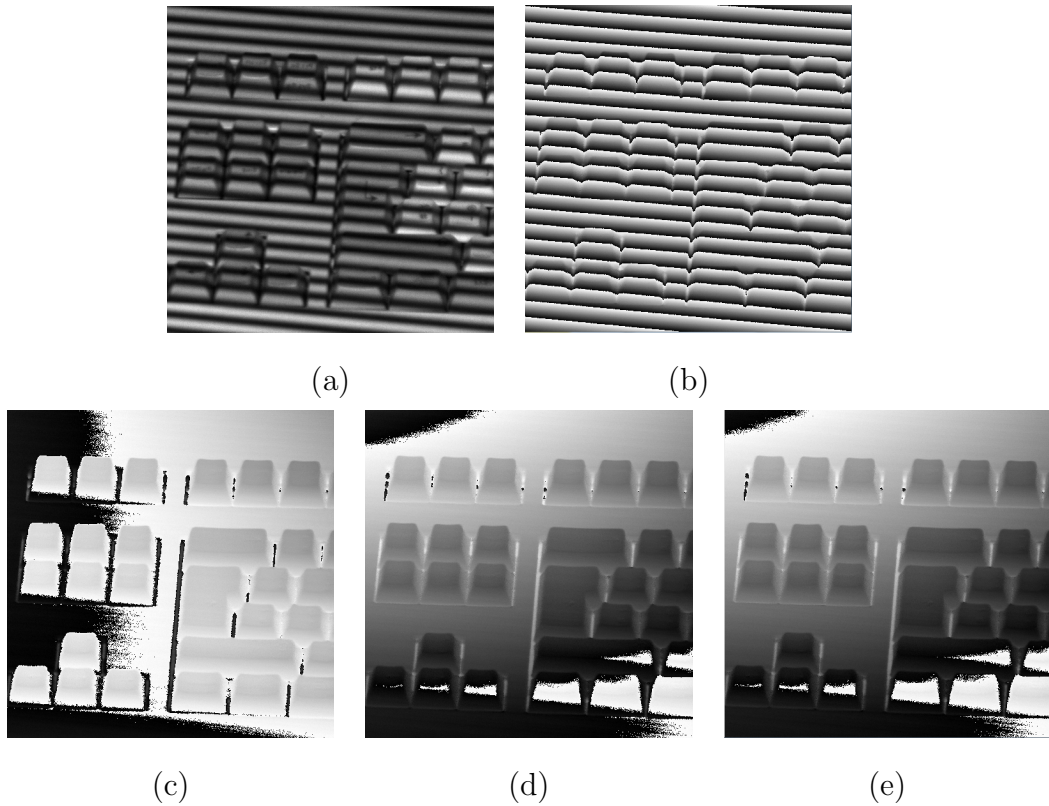


Figure 6: (a) A real fringe pattern, (b) corresponding wrapped phase signal, and results obtained by (c) frequency shifting in Fourier space; (d) spatial method using interpolation on highest frequency bin; and (e) spatial method using average of samples in highest frequency bin

ilar for the wrapped phase signals that are shown in Figures 6(b) and 8(b). In both of these cases the three methods leave a single wrap in the resulting phase map. However, there are observable differences in the results that were obtained for Figure 7(b). In this case, the frequency shift method has managed to remove most of the carrier frequency, leaving only a residual tilt. In contrast it can be seen that the proposed spatial method has actually left a remnant of the carrier frequency, but significantly it has further reduced

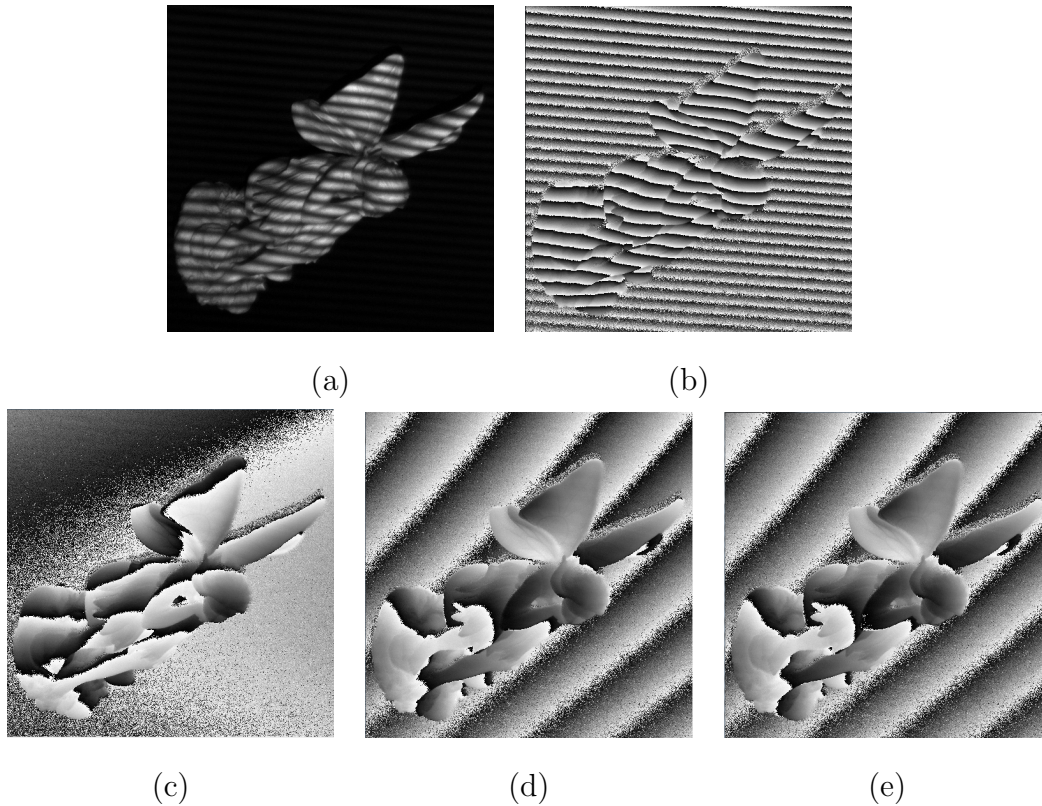


Figure 7: (a) A real fringe pattern, (b) corresponding wrapped phase signal, and results obtained by (c) frequency shifting in Fourier space; (d) spatial method using interpolation on highest frequency bin; and (e) spatial method using average of samples in highest frequency bin

the number of fringes on the actual area of interest.

In all the examples shown in this section, a residual tilt of a similar magnitude can be observed in the result. In the case of the frequency shift method, shifts can only be measured in terms of an integer number of pixels. This causes a residual phase, unless the fringe frequency has an exact integer value in both the x and y directions [22]. In the case of the spatial methods being proposed, the difference between the real mode and the estimate causes

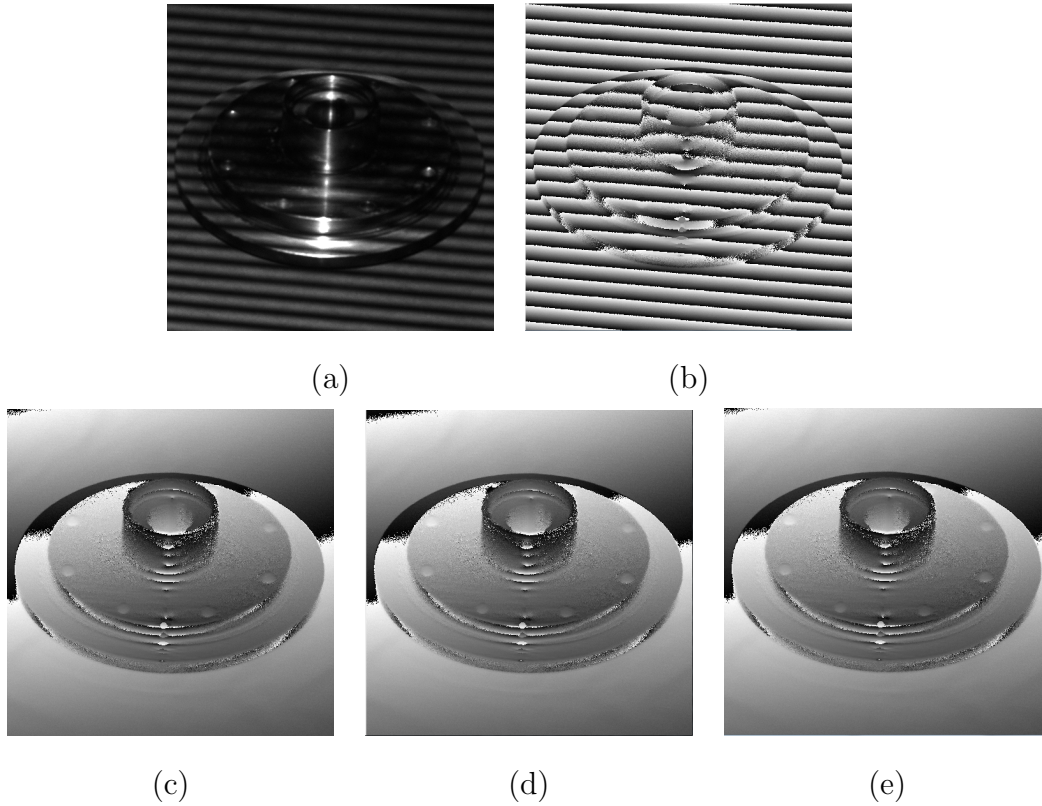


Figure 8: (a) A real fringe pattern, (b) corresponding wrapped phase signal, and results obtained by (c) frequency shifting in Fourier space; (d) spatial method using interpolation on highest frequency bin; and (e) spatial method using average of samples in highest frequency bin

a similar effect.

4.2. Impact of the wrap reduction

As a second task, we have run an experiment to globally assess the impact of a wrap reduction before the unwrapping operation. In particular, we have used the wrapped phase signal shown in Figure 5(a) to evaluate the impact of the application of the wrap reduction method on the unwrapping result.

Figures 9(a) and (b) illustrate the results using best path unwrappers[13] with two different quality measures, namely the maximum absolute gradient[23], and the first phase difference[24]. To improve the visibility of the results, a convenient slope has been artificially subtracted after unwrapping. Despite the apparent simplicity, this signal is relatively complex to unwrap, and an incorrect unwrapping is observed in both cases. On the other hand, the original signal is correctly retrieved when the same unwrapping methods are applied upon the signals with reduced wraps, shown in Figures 5(b)-(d). Figure 9(c) shows the result when the maximum gradient is applied to Figure 5(c), but there is no observable difference when Figure 5(b) or (d) are used, or when applying the first phase difference as the quality measure. In all cases, the application of the wrap reduction method has altered the first differences in the original phase signal, and helped in the process of building a more reliable quality map that is reflected in the improved final unwrapping result.

4.3. Execution time

In order to evaluate the comparative computational performance of the methods, we ran a last test. All three algorithms have been implemented in Matlab, and executed in single thread mode on artificial wrapped phase signals of various sizes. All signals had the same number of rows as columns ($n = 2^i, i \in [4, 5, \dots, 13]$), giving problem sizes of $n \times n = 4^i, i \in [4, 5, \dots, 13]$.

The experiment was run on a machine with an Intel Core i7 CPU 930 running at 2.80 GHz and with 8 Gbyte of RAM. When a single execution did

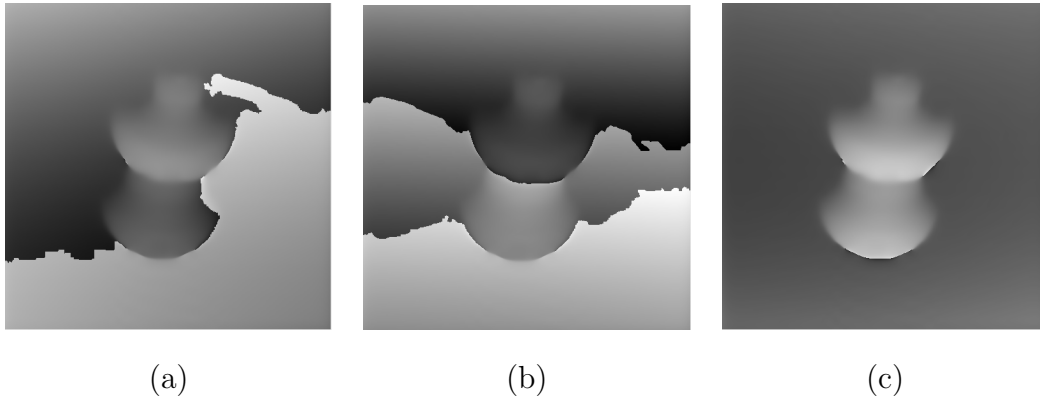


Figure 9: Result of unwrapping before and after applying the wrap reduction method: (a) best path unwrapper on original signal, using absolute gradient; (b) best path unwrapper on original signal, using first phase difference; and (c) result after the application of the wrap reduction method proposed

not allow for an accurate measurement, times were averaged over a number of runs. Table 1 shows the running time for the three methods, as a function of the size of the problem (rows *times* columns). Larger sizes are not reported because the trend was already observable at this point and some of the algorithms started to suffer from memory problems.

The HIM algorithm runs the fastest in all cases. This is because all operations are linear with the signal size and the method requires a single pass to estimate the mode. The HAM version has a slightly higher cost, mainly due to the second pass that is required to filter signal values in the most frequent histogram bin. In all cases, the frequency shift method is clearly the slowest, despite the highly efficient implementation that is available in Matlab. It can also be observed that percentage differences increase noticeably for the largest sizes, because of the $O(n^2 \log n)$ computational cost of the FFT. For a size 8192×8192 the two spatial methods run in less than half the time of

size	HIM	HAM	Frequency shift
16×16	0.0003	0.0003	0.0003
32×32	0.0004	0.0005	0.0007
64×64	0.0008	0.0010	0.0018
128×128	0.0029	0.0031	0.0064
256×256	0.0100	0.0168	0.0261
512×512	0.0338	0.0392	0.0762
1024×1024	0.1234	0.1500	0.2428
2048×2048	0.5339	0.6304	0.9255
4096×4096	2.1605	2.5632	3.8614
8192×8192	9.7949	11.3606	22.7531

Table 1: Running time for the three methods, in seconds

the frequency shift approach.

It is also worth noticing that the execution time for both the frequency shifting approach and the HIM version of the proposed algorithm does not depend on the particular image that is being unwrapped. Signal dependency in the case of the HAM version of the proposed method is also relatively low, as it only applies to the computation of the average of the phase values in the most frequent bin. This is just a small fraction of the overall measurement algorithm execution time and has a cost of $O(n)$, which is bounded by the worst case that happens when all values fall within the same bin.

5. Discussion and Conclusions

In this paper, we have introduced a novel technique for phase wrap reduction in fringe projection profilometry. The algorithm can be used as an aid to phase unwrapping, and performs significantly faster than existing methods based on frequency shifting in the Fourier domain [3, 18, 19] when using phase extraction methods other than Fourier Analysis. Additional computational gains to the ones reported in this paper can be achieved by restricting the range of slopes that are considered by the algorithm. This would allow discarding all first differences above a certain threshold, and could potentially yield further reductions of the computation times that are reported in Table 1.

Another aspect to consider is the presence of high levels of noise in the wrapped phase signals. Although we have successfully applied the method to noisy signals, there are specific situations where the frequency shifting method can potentially yield better results. One such example is in speckle interferometry. When the noise has a high frequency, it appears as a well localized noise component in the Fourier spectrum, usually far away from the required phase signal information in terms of its position in Fourier space. As long as the noise does not become the predominant frequency, the frequency shift method remains immune to such noise. On the contrary, the inherent locality of the proposed spatial method does not provide such an immunity to dense high frequency noise. When a filtering stage is used as part of the phase extraction process from a speckle pattern, it is highly advisable that filtering is applied before any wrap reduction, rather than afterwards, so as to increase the robustness of the result.

Acknowledgments

Authors would like to thank the Spanish Ministry of Economy and Competitiveness for the funding received through projects TIN2011-29221-C03-02 and TIN2014-59641-C2-1-P.

References

- [1] Z. Zhang, Z. Jing, Z. Wang, D. Kuang, Comparison of Fourier transform, windowed Fourier transform, and wavelet transform methods for phase calculation at discontinuities in fringe projection profilometry, *Optics and Lasers in Engineering* 50 (8) (2012) 1152 – 1160, fringe Analysis Methods and Applications.
- [2] C. Quan, W. Chen, C. Tay, Phase-retrieval techniques in fringe-projection profilometry, *Optics and Lasers in Engineering* 48 (2) (2010) 235 – 243, fringe Projection Techniques.
- [3] M. Takeda, H. Ina, S. Kobayashi, Fourier-transform method of fringe-pattern analysis for computer-based topography and interferometry, *Journal of the Optical Society of America* 72 (1) (1982) 156–160.
- [4] J. Zhong, J. Weng, Phase retrieval of optical fringe patterns from the ridge of a wavelet transform, *Optics Letters* 30 (19) (2005) 2560–2562.
- [5] M. Gdeisat, D.R. Burton, F. Lilley, M. Arevalillo-Herráez, Fast fringe pattern phase demodulation using FIR Hilbert transformers, *Optics Communications* 359 (2016) 200–206.

- [6] B. Li, C. Tang, Shearlet transform for phase extraction in fringe projection profilometry with edges discontinuity, *Optics and Lasers in Engineering* 78 (2016) 91–98.
- [7] K. Perry Jr, J. McKelvie, A comparison of phase shifting and Fourier methods in the analysis of discontinuous fringe patterns, *Optics and Lasers in Engineering* 19 (45) (1993) 269 – 284.
- [8] Z. Zhao, H. Zhao, L. Zhang, F. Gao, Y. Qin, H. Du, 2D phase unwrapping algorithm for interferometric applications based on derivative Zernike polynomial fitting technique, *Measurement Science and Technology* 26 (1) (2015) 017001.
- [9] M. Rivera, F. J. Hernandez-Lopez, A. Gonzalez, Phase unwrapping by accumulation of residual maps, *Optics and Lasers in Engineering* 64 (2015) 51 – 58.
- [10] Q. Huang, H. Zhou, S. Dong, S. Xu, Parallel branch-cut algorithm based on simulated annealing for large-scale phase unwrapping, *IEEE Transactions on Geoscience and Remote Sensing* 53 (7) (2015) 3833–3846.
- [11] D. Zheng, F. Da, A novel algorithm for branch cut phase unwrapping, *Optics and Lasers in Engineering* 49 (5) (2011) 609 – 617.
- [12] H. Zhong, J. Tang, S. Zhang, Phase quality map based on local multi-unwrapped results for two-dimensional phase unwrapping, *Applied Optics* 54 (4) (2015) 739–745.
- [13] M. Arevalillo Herráez, D. R. Burton, M. J. Lalor, M. A. Gdeisat, Fast

- two-dimensional phase-unwrapping algorithm based on sorting by reliability following a noncontinuous path, *Applied Optics* 41 (35) (2002) 7437–7444.
- [14] K. Chen, J. Xi, Y. Yu, Quality-guided spatial phase unwrapping algorithm for fast three-dimensional measurement, *Optics Communications* 294 (2013) 139 – 147.
- [15] G. Liu, R. Wang, Y. Deng, R. Chen, Y. Shao, Z. Yuan, A new quality map for 2-D phase unwrapping based on gray level co-occurrence matrix, *IEEE Geoscience and Remote Sensing Letters* 11 (2) (2014) 444–448.
- [16] C. Ojha, M. Manunta, A. Pepe, L. Paglia, R. Lanari, An innovative region growing algorithm based on minimum cost flow approach for phase unwrapping of full-resolution differential interferograms, in: *IEEE International Conference on Geoscience and Remote Sensing Symposium (IGARSS)*, 2012, pp. 5582–5585.
- [17] M. Arevalillo Herráez, J. G. Boticario, M. J. Lalor, D. R. Burton, Agglomerative clustering-based approach for two-dimensional phase unwrapping, *Applied Optics* 44 (7) (2005) 1129–1140.
- [18] D. R. Burton, A. J. Goodall, J. T. Atkinson, M. J. Lalor, The use of carrier frequency shifting for the elimination of phase discontinuities in Fourier transform profilometry, *Optics and Lasers in Engineering* 23 (4) (1995) 245 – 257.
- [19] M. Qudeisat, M. Gdeisat, D. Burton, F. Lilley, A simple method for

- phase wraps elimination or reduction in spatial fringe patterns, *Optics Communications* 284 (21) (2011) 5105 – 5109.
- [20] D. R. Bickel, R. Frhwirth, On a fast, robust estimator of the mode: Comparisons to other robust estimators with applications, *Computational Statistics & Data Analysis* 50 (12) (2006) 3500 – 3530.
- [21] J. Jing, I. Koch, K. Naito, Polynomial histograms for multivariate density and mode estimation, *Scandinavian Journal of Statistics* 39 (1) (2012) 75–96.
- [22] T. J. McIntyre, A. I. Bishop, Fringe-a java-based finite fringe analysis package, *Computer Physics Communications* 183 (9) (2012) 2014 – 2018.
- [23] D. C. Ghiglia, M. D. Pritt, *Two-Dimensional Phase Unwrapping: Theory, Algorithms, and Software*, Wiley, New York, 1998.
- [24] X. Su, W. Chen, Reliability-guided phase unwrapping algorithm: a review, *Optics and Lasers in Engineering* 42 (3) (2004) 245–61.